J Neurophysiol 102: 203–213, 2009.
First published April 22, 2009; doi:10.1152/jn.91158.2008.

Synergistic Roles of $GABA_A$ Receptors and SK Channels in Regulating Thalamocortical Oscillations

Max Kleiman-Weiner,[1] Mark P. Beenhakker,[2] William A. Segal,[2] and John R. Huguenard[2]
Departments of [1]Biological Sciences and [2]Neurology and Neurological Sciences, Stanford University, Stanford, California

Submitted 17 October 2008; accepted in final form 15 April 2009

Kleiman-Weiner M, Beenhakker MP, Segal WA, Huguenard JR. Synergistic roles of $GABA_A$ receptors and SK channels in regulating thalamocortical oscillations. *J Neurophysiol* 102: 203–213, 2009. First published April 22, 2009; doi:10.1152/jn.91158.2008. Rhythmic oscillations throughout the cortex are observed during physiological and pathological states of the brain. The thalamus generates sleep spindle oscillations and spike-wave discharges characteristic of absence epilepsy. Much has been learned regarding the mechanisms underlying these oscillations from in vitro brain slice preparations. One widely used model to understand the epileptiform oscillations underlying absence epilepsy involves application of bicuculline methiodide (BMI) to brain slices containing the thalamus. BMI is a well-known $GABA_A$ receptor blocker that has previously been discovered to also block small-conductance, calcium-activated potassium (SK) channels. Here we report that the robust epileptiform oscillations observed during BMI application rely synergistically on both $GABA_A$ receptor and SK channel antagonism. Neither application of picrotoxin, a selective $GABA_A$ receptor antagonist, nor application of apamin, a selective SK channel antagonist, alone yielded the highly synchronized, long-lasting oscillations comparable to those observed during BMI application. However, partial blockade of SK channels by subnanomolar concentrations of apamin combined with picrotoxin sufficiently replicated BMI oscillations. We found that, at the cellular level, apamin enhanced the intrinsic excitability of reticular nucleus (RT) neurons but had no effect on relay neurons. This work suggests that regulation of RT excitability by SK channels can influence the excitability of thalamocortical networks and may illuminate possible pharmacological treatments for absence epilepsy. Finally, our results suggest that changes in the intrinsic properties of individual neurons and changes at the circuit level can robustly modulate these oscillations.

INTRODUCTION

Neural network oscillations are observed during both normal and pathological states of the brain. Coherent oscillatory activity that is synchronized throughout the cortex is often driven by the thalamus, a subcortical structure. Examples of such activity include both the 7- to 14-Hz spindle oscillations observed during sleep (McCormick and Bal 1997) and the characteristic 3-Hz spike-wave seizures of the neurological disorder, absence epilepsy (McCormick and Contreras 2001).

Thalamocortical oscillations arise from reciprocal connectivity between inhibitory GABAergic neurons in the reticular nucleus (RT) of the thalamus and excitatory thalamocortical relay neurons. During these oscillations, RT neurons release GABA onto relay neurons activating $GABA_A$ and $GABA_B$ receptors. This action hyperpolarizes relay neurons and provides the necessary stimulus to prime T-type calcium channels. Once the actions of GABA have subsided, relay neurons depolarize and fire postinhibitory rebound, T-type calcium channel-dependent bursts of action potentials (Huguenard and Prince 1994), resulting in the re-excitation of RT neurons. This relay-to-RT neuron excitation is mediated by both α-amino-3-hydroxy-5-methyl-4-isoxazolepropionic acid (AMPA) and *N*-methyl-D-aspartic acid (NMDA) glutamate receptors and is responsible for initiating the subsequent cycle of the oscillation (Huguenard and McCormick 2007; von Krosigk et al. 1993).

An important component of thalamic circuitry that suppresses network hyperexcitability is RT-to-RT neuron inhibition (Huntsman et al. 1999). Indeed, a well-studied rodent brain slice model indicates that reduced intra-RT inhibition enhances RT neuron excitability and leads to the generation of ~3-Hz oscillatory activity characteristic of absence epilepsy (Sohal et al. 2000). Specifically, application of bicuculline methiodide (BMI), a $GABA_A$ receptor antagonist, to such slices produces robust epileptiform oscillations by presumably reducing intra-RT inhibition (Huguenard and Prince 1994; von Krosigk et al. 1993). In vivo, BMI infusion directly into the rat thalamus also results in 3-Hz synchronous thalamocortical oscillations (Castro-Alamancos 1999). However, previous work showed that, in addition to its synaptic action—antagonism of $GABA_A$ receptor dependent synaptic inhibition—BMI has direct effects on intrinsic excitability including block of small-conductance, calcium-activated potassium (SK) channels (Debarbieux et al. 1998). This finding leads to the possibility that one or both actions of BMI are necessary to generate epileptiform activity in this slice model.

SK channels are voltage invariant and are activated solely by intracellular calcium ions (Schumacher et al. 2001). They link the tightly regulated intracellular calcium concentration to membrane potential by hyperpolarizing the neuron on activation and can strongly influence intrinsic cell firing properties and calcium transients (Stocker 2004). Localization studies show that the thalamic reticular nucleus expresses a high density of SK2 subunits as well as a lower density of SK1 and SK3 subunits, which, when coassembled as multimers, form channels that display a high affinity for apamin, a selective SK channel antagonist (Debarbieux et al. 1998; Sailer et al. 2002, 2004). Elucidating the combined BMI actions of $GABA_A$ receptor and SK channel antagonism that promote epileptiform activity will provide a better understanding of human absence epilepsy and illuminate possible pharmacological treatments for this disease. Here we report that the robust epileptiform oscillations observed during BMI application rely on both $GABA_A$ receptor and SK channel antagonism.

Address for reprint requests and other correspondence: J. R. Huguenard, Dept. of Neurology and Neurological Sciences, Rm. M030 Alway Bldg., Stanford Univ. School of Medicine, Stanford, CA 94305-5122 (E-mail: John.Huguenard@stanford.edu).

METHODS

Slice preparation

All procedures involving animals were performed in accordance with protocols approved by the Stanford University Institutional Animal Care and Use Committee. Sprague-Dawley rats (P10–P16) were anesthetized with pentobarbital sodium (55 mg/kg) and decapitated. The brains were rapidly extracted and placed in chilled (4°C) oxygenated slicing solution containing (in mM) 234 sucrose, 26 $NaHCO_3$, 11 glucose, 10 $MgSO_4$, 2.5 KCl, 1.25 NaH_2PO_4, and 0.5 $CaCl_2$ equilibrated with a 95% O_2-5% CO_2 mixture. Horizontal slices (400 μm) containing thalamus were obtained with a vibratome (Leica Microsystems, Bannockburn, IL), and hippocampus and cortex were removed. The slices were incubated at 34°C for 1 h in oxygenated saline consisting of (in mM) 126 NaCl, 26 $NaHCO_3$, 10 glucose, 2.5 KCl, 2 $CaCl_2$, 1.25 NaH_2PO_4, and 1 $MgSO_4$ and maintained at room temperature. In our extracellular recording configuration, apamin washed in very slowly so most slices were incubated in apamin at room temperature for 20–40 min before experimentation.

Extracellular multiunit recordings

Slices were placed in an interface chamber at 34°C and perfused with oxygenated saline. Electrical stimuli were delivered to the internal capsule through a pair of 50- to 100-KΩ bipolar tungsten electrodes (FHC, Bowdoinham, ME), with a separation of ~100 μm. Extracellular multiunit recordings were made with 50- to 100-KΩ tungsten electrodes placed in the RT and were band-pass filtered between 100-Hz and 3-kHz. Recordings were obtained and digitized with a Digidata 1200 and pClamp software (Axon Instruments, Foster City, CA). The bursting activity recorded by our extracellular electrodes corresponds to a population burst that is composed of activity from multiple neurons, each bursting with different onset times and durations.

Intracellular recordings

All intracellular recordings were performed in a submerged chamber in which 300-μm-thick slices situated on nylon netting were continuously perfused with warm (34°C) oxygenated physiological saline (2 ml/min). Intracellular, current-clamp recordings in the submerged chamber were made using visualized techniques in the whole cell patch-clamp configuration. Intracellular recording pipettes were created by pulling borosilicate capillary glass (Sutter Instruments, Novato, CA) with a P80 puller (Sutter Instruments) and had 1- to 2-MΩ tip resistances. Potassium gluconate–based pipette solution was used and contained (in mM) 100 K-gluconate, 13 KCl, 10 EGTA, 10 HEPES, 9 $MgCl_2$, $2Na_2ATP$, and 0.5 NaGTP, 0.07 $CaCl_2$. Pipette solutions were adjusted to have a pH of 7.4 and an osmolarity of 280–285 mosm/l. The junction potential was corrected for. Recordings were obtained with a Multiclamp 700A amplifier (Axon Instruments) and digitized/acquired onto computer with a Digidata 1322A acquisition system (Axon Instruments) using pClamp software. To assess neuronal excitability, we delivered a family of current injections (−200 to +200pA in 50-pA increments for 400 ms) and measured the number of action potentials generated and the action potential frequency. We maintained neurons at a membrane potential near −60 mV by adjusting the bias current. We observed a trend for greater change in bias current with higher apamin concentrations, but the change was not significant. To compensate for electrode resistance, we balanced out the associated voltage drop using the bridge circuit on the amplifier. All intracellular recordings had an access resistance <20 MΩ.

Data analysis

To find spikes in extracellular multiunit recordings, we used software previously described (Sohal et al. 2003). In brief, spikes were detected as steep slope deflections two- to three-fold greater than the root-mean-square of the background noise in each recording. Individual spikes were characterized by a rapid rise and descent within a 5-ms interval. Spikes were binned every 10 ms into histograms. From this spike rate histogram, an autocorrelogram for each sweep was generated using the MATLAB signal processing toolkit. Peaks and troughs were detected using a filtered autocorrelogram. The oscillation index (OI), a measure of oscillatory synchrony, was determined by calculating the average amplitude of the first two oscillatory peaks ($P_{1,2}$) from the autocorrelogram and then subtracting the amplitude of the trough (T) between them. This result is divided by the average amplitude of those first two peaks $\left(\mathrm{OI} = \frac{(P_{12} - T)}{P_{12}}\right)$. The duration of an oscillation was quantified by the interval between the stimulus and the last rhythmic burst of the oscillation (Sohal et al. 2003). The last burst was determined by the last two consecutive bins in the spike rate histogram that contained more than five spikes and occurred within 1 s of the last detected bin with more than five spikes. The period of the oscillation was determined from the first peak of the autocorrelogram after the zero time point (Sohal et al. 2003). Dose dependency of apamin's effects was shown by linear regression. Statistical significance is reported as regression ANOVA. Comparisons between two groups were tested with paired or two-sample *t*-test as noted.

For intracellular recordings, spikes were detected by threshold with hysteresis in Clampfit 9.2 (Axon Instruments). The duration of the burst was calculated by the time between the first spike and last spike, and the mean spike frequency was calculated by the number of spikes divided by the burst duration. In neurons in which depolarizing current injection led to mixed mode firing, all spikes were counted.

RESULTS

$GABA_A$ receptor antagonism alone does not reproduce BMI oscillations

Determining the actions of BMI in the thalamus will show how this pharmacological agent promotes the generation of 3-Hz epileptiform activity in widely used in vitro (Huguenard and McCormick 2007; von Krosigk et al. 1993) and in vivo (Castro-Alamancos 1999) models of absence epilepsy. Therefore we performed experiments designed to parse out the dual actions of BMI, $GABA_A$ receptor antagonism (a synaptic or extrinsic effect) and SK channel antagonism (an effect on intrinsic excitability). We used picrotoxin (PTX) to selectively block $GABA_A$ receptors and apamin to block SK channels. Because BMI concentrations of 10 μM are often used to generate epileptiform activity (Huguenard and Prince 1994), we used a concentration of PTX that yields comparable $GABA_A$ receptor blockade. Because 10 μM BMI only partially blocks SK channels (Strobaek et al. 2000), we used multiple concentrations of apamin (0.3, 1, and 10 nM) to cover a range of blockade efficacies. We first tested whether either action of BMI alone can sufficiently replicate BMI-like oscillations.

To test the sufficiency of $GABA_A$ receptor blockade in replicating BMI-like oscillations, we used 50 μM PTX, a $GABA_A$ receptor antagonist with no known actions on SK channels (Debarbieux et al. 1998). PTX (50 μM) is equally effective as 10 μM BMI in blocking $GABA_A$ receptor–mediated inhibition (Pisani et al. 2002). In control conditions, electrical stimulation of the internal capsule elicited a fast spindle-like oscillation (Jacobsen et al. 2001) characterized by a relatively short period (100–200 ms) and a low proportion of synchronized activity (Fig. 1*A*). Application of either BMI

($n = 14$) or PTX ($n = 10$) transformed spindle activity into epileptiform oscillations (Fig. 1*B*). Although BMI and PTX both altered spindle oscillations, the actions of the two antagonists were different. To quantify these differences, we constructed autocorrelograms from spike rate histograms of spikes detected during the evoked oscillation (Fig. 1*C*; see METHODS).

We used four parameters to describe the properties of evoked oscillations. *1*) Oscillation index: OI is a measure of oscillation strength and is calculated by determining the peak-to-valley ratio of the autocorrelogram. *2*) Oscillation duration: this parameter is measured as the time between the stimulus and the termination of the last burst of the oscillation. *3*) General activity: this is a measure of the total number of action potentials per oscillation. *4*) Oscillation period: this period is the average interval between bursts. A robust epileptiform oscillation with features consistent with absence epilepsy was considered to have high synchrony (i.e., high oscillation index), a long duration, a high spike count, and a period between 300 and 500 ms to match the period commonly seen in absence spike wave discharges.

On average, oscillations in BMI had a significantly higher OI (0.81 ± 0.05 vs. 0.61 ± 0.09, *t*-test, $P < 0.05$), lasted longer (4.6 ± 0.5 vs. 1.9 ± 0.3 s, *t*-test, $P < 0.001$), had more spikes (971 ± 144 vs. 367 ± 52, *t*-test, $P < 0.01$), and had a slightly shorter interburst interval (377 ± 10 vs. 346 ± 11 ms, *t*-test, $P < 0.05$) than oscillations in PTX (Fig. 1*D*). From these results, we concluded that, although PTX transformed spindles into epileptiform oscillations, $GABA_A$ receptor blockade alone could not fully account for the robust oscillation (characterized by a long duration and high oscillation synchrony) observed during BMI application.

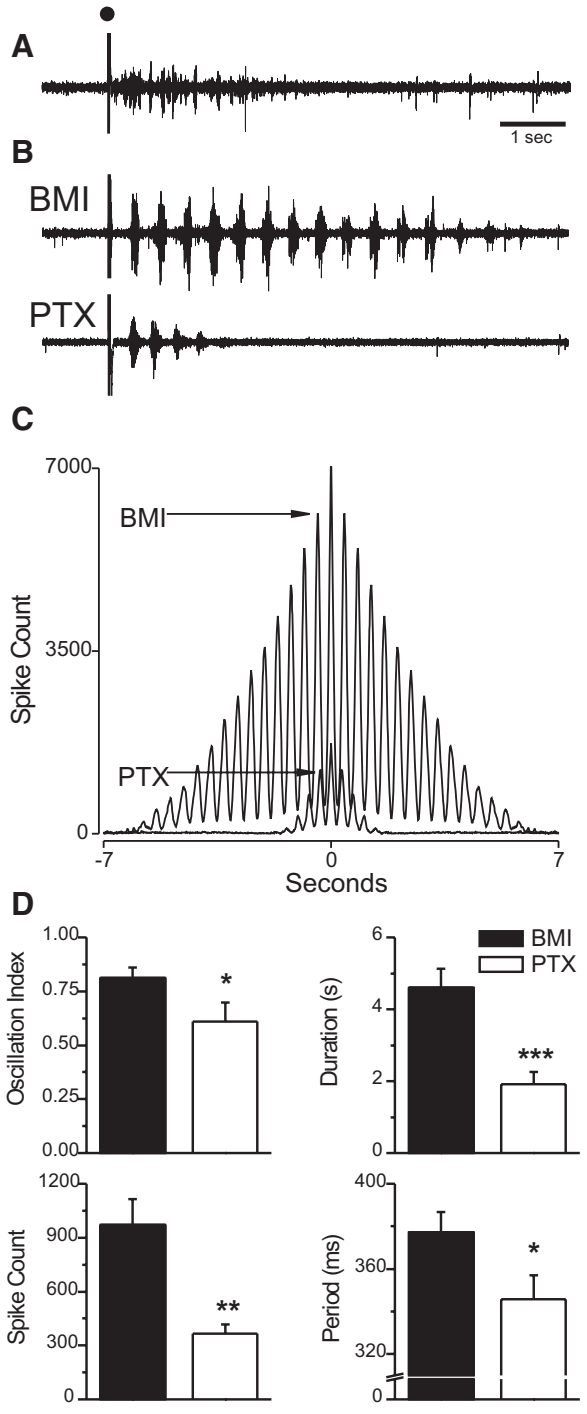

FIG. 1. $GABA_A$ receptor antagonism alone does not reproduce bicuculline methiodide (BMI) oscillations. *A*: stimulating corticothalamic fibers under control conditions evokes a spindle-like oscillation in the in vitro thalamic slice preparation. Shown is a recording from an extracellular electrode placed in the reticular nucleus (RT) nucleus during an evoked oscillation, which persisted for a few seconds. Dot marks stimulation. *B*: bath application of either $GABA_A$ receptor antagonist, BMI 10 μM (*top*), or picrotoxin (PTX) 50 μM (*bottom*) transformed spindle-like activity into a slow epileptiform synchronized oscillation (recordings are from 2 different slices). *C*: evoked oscillations in *B* were quantified by generating autocorrelograms from spike rate histograms. This analysis showed the rhythmic bursting patterns of BMI and PTX oscillations. Arrows point to the 1st oscillatory peak of the autocorrelograms, which was used to calculate the period and oscillatory index. *D*: summary plots show quantitative differences in BMI- ($n = 14$, black bars) and PTX- ($n = 10$, white bars) induced oscillations. Oscillations in the presence of PTX are briefer, have a shorter period, contain fewer spikes, and are less synchronized as measured by the oscillation index (*t*-test: $*P < 0.05$; $**P < 0.01$; $***P < 0.001$).

SK channel antagonism alone does not produce robust epileptiform oscillations

Because $GABA_A$ receptor antagonism (PTX) did not replicate the effects of BMI, we next determined whether the characteristic robust epileptiform oscillation caused by BMI was caused by SK channel antagonism, another target of BMI. We used multiple concentrations of apamin [0.3 ($n = 8$), 1 ($n = 6$), and 10 nM ($n = 6$)] to cover a range of blockade efficacies and recorded their effects on the spindle-like oscillations (Fig. 2*A*). Apamin (10 nM) provides a near complete blockade of SK channels (Strobaek et al. 2000).

All concentrations of apamin we tested altered the properties of spindle oscillations (Fig. 2*C*). Furthermore, apamin prolonged the oscillation in a dose-dependent manner (control: 3.6 ± 0.8 s, 0.3 nM: 4.7 ± 1.0 s, 1 nM: 5.5 ± 1.0 s, 10 nM: 8.1 ± 1.8 s; regression ANOVA, $P < 0.05$). Apamin also increased the period of the oscillations (control: 162 ± 7 ms, 0.3 nM: 167 ± 9 ms, 1 nM: 210 ± 30 ms, 10 nM: 306 ± 14 ms; regression ANOVA, $P < 0.0001$), and there was more general activity (control spikes: 660 ± 144, 0.3 nM: 1004 ± 195, 1 nM: 890 ± 122, 10 nM: 1587 ± 339; regression ANOVA, $P < 0.01$). When applied alone, a high concentration of apamin (10 nM) resulted in an oscillation period similar to that observed in BMI (10 nM apamin: 306 ± 14 ms; BMI:

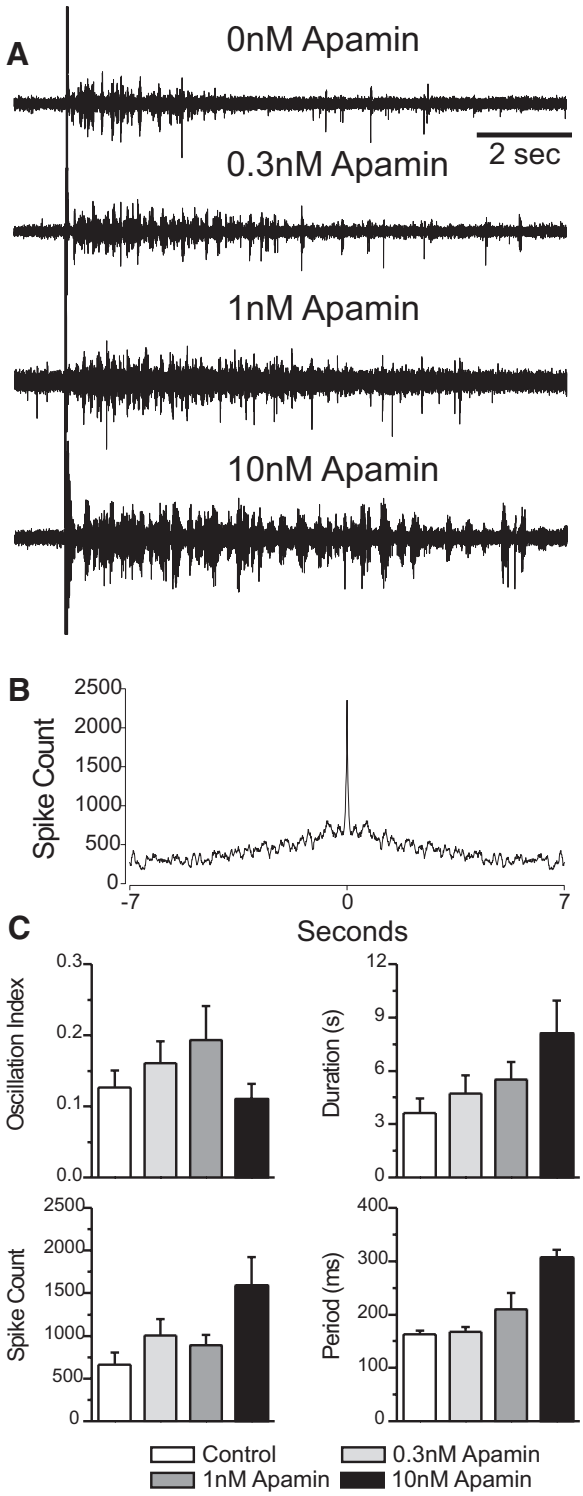

FIG. 2. Small-conductance, calcium-activated potassium (SK) channel antagonism alone does not produce robust epileptiform oscillations. *A*: representative extracellular recordings from different slices show the effect of bath application of various concentrations of apamin (0–10 nM) on evoked oscillations. *B*: a representative autocorrelogram of an evoked oscillation in the presence of 10 nM apamin. *C*: increases in apamin concentration [0.3 ($n = 8$), 1 ($n = 6$), and 10 nM ($n = 6$)] were associated with increases in duration, period, and number of spikes in evoked oscillations. In contrast, whereas 0.3 and 1 nM apamin produced slight increases in oscillatory indices, these were not further augmented by increasing apamin concentration to 10 nM, and in general, oscillatory indices remained far lower than those associated with BMI application (cf. Fig. 1*D*; OI > 0.8).

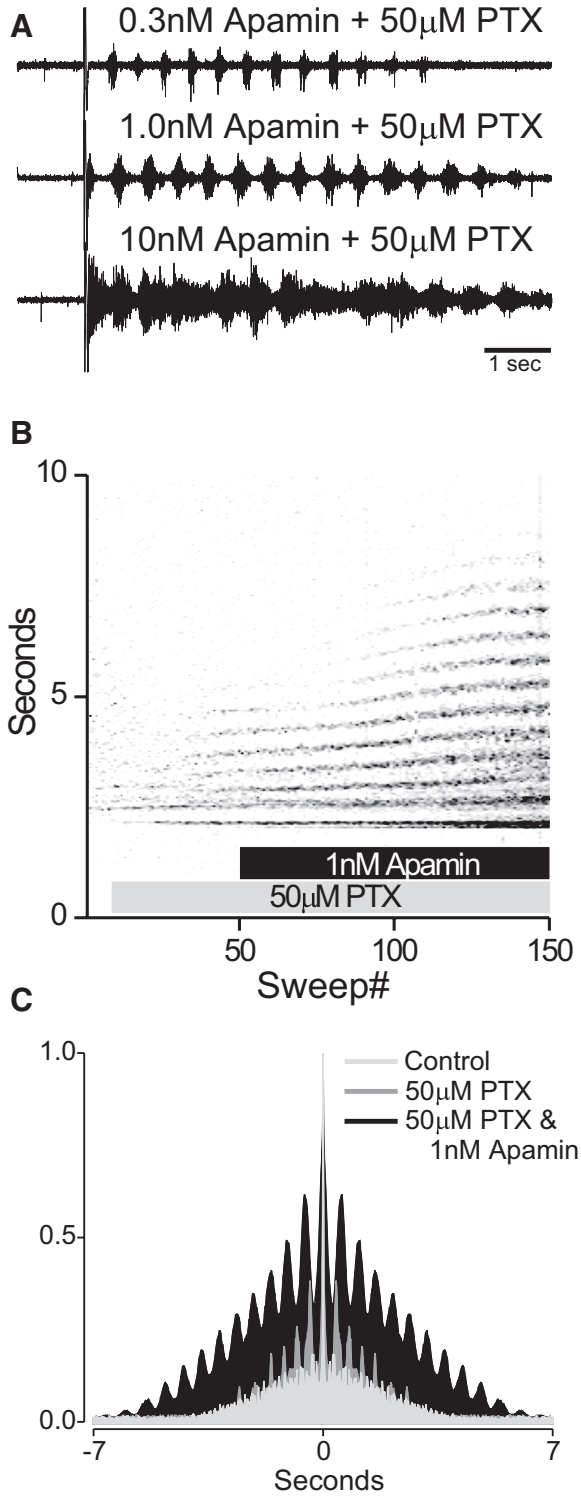

FIG. 3. Partial SK channel blockade enhances PTX oscillations. *A*: evoked oscillations during coapplication of apamin (0.3, 1, and 10 nM) and PTX generated a robust 3-Hz oscillation. Partial (0.3 or 1 nM) SK channel antagonism yielded more synchronized activity patterns. In contrast, a high concentration of apamin (10 nM) yielded nearly continuous asynchronous sustained firing. *B*: contour plot showing evoked oscillatory activity during a 10-s recording period from a single slice. The contours represent spike rate per 10 ms, with black representing the highest rate. Note the prolongation and slowing of the PTX oscillation on the addition of apamin. *C*: 3 overlapping autocorrelograms show the effect of PTX (gray) on spindle-like oscillations (light gray) and combined effect of apamin (1 nM) and PTX (black).

377 ± 10 ms). However, although 10 nM apamin yielded oscillations that most closely approximated BMI in number of spikes, duration, and period, the resulting oscillations lacked the robust synchrony of the BMI oscillations as measured by oscillation indices (OI 10 nM apamin, 0.11 ± 0.02; OI BMI, 0.81 ± 0.05; *t*-test, $P < 0.0001$; Fig. 2*C*). Thus no concentration of apamin produced oscillations with similar synchrony to a BMI or PTX oscillation, i.e., in apamin alone the oscillations remained spindle-like in terms of synchrony. From these results, we concluded that apamin alone does not replicate evoked BMI oscillations and does not generate highly synchronized epileptiform oscillations. However, these results do show that apamin can affect some properties of spindles.

$GABA_A$ receptor antagonism and partial SK channel blockade combined replicate robust BMI oscillations

In the previous two experiments, we showed that neither PTX nor apamin alone was sufficient for robust BMI-like oscillations. From these results, we hypothesized that both targets of BMI contribute to the characteristic epileptiform activity evoked in this model of absence epilepsy. To test this hypothesis, we determined whether blockade of $GABA_A$ receptor–mediated inhibition combined with partial blockade of SK channels by the various concentrations of apamin could replicate BMI-like oscillations.

In the presence of PTX, we applied one of three concentrations of apamin [0.3 ($n = 11$), 1 ($n = 11$), and 10 nM ($n = 4$)]. Apamin had robust effects on the PTX-evoked oscillations (Fig. 3). An example from a single experiment showing the effect of 1 nM apamin on PTX-induced oscillations is shown in Fig. 3*B*. We observed two outcomes. The lower concentrations of apamin (0.3 and 1 nM) combined with PTX (50 μM) enhanced the synchrony (0.3 nM OI: 0.74 ± 0.05, 1 nM OI: 0.80 ± 0.05), prolonged the duration (0.3 nM: 3.7 ± 0.6 s, 1 nM: 4.8 ± 0.8 s), and increased the period (0.3 nM: 384 ± 14 ms, 1 nM: 414 ± 16 ms) and number of spikes (0.3 nM: 753 ± 130, 1 nM: 1012 ± 180) of the oscillations to BMI-like levels (Fig. 4). The highest concentration of apamin (10 nM) produced long-lasting oscillations (10 nM: 7.4 ± 0.7 s; *t*-test, $P < 0.05$), with many more spikes (10 nM: 3,785 ± 345; *t*-test, $P < 0.0001$) and less synchrony (10 nM OI: 0.07 ± 0.02; *t*-test, $P < 0.0001$) than the lower concentration of apamin conditions (Figs. 3*A* and 4). These results show that both actions of BMI, $GABA_A$ receptor and SK channel antagonism contribute to the generation of robust epileptiform oscillations characteristic of absence epilepsy.

Prior $GABA_A$ receptor and SK channel blockade largely occludes BMI-mediated transformation of thalamic oscillation

Although we replicated the effects of BMI with a combination of PTX and apamin, it is possible that BMI has other unknown pharmacological targets that may affect the oscillatory activity (Olsen et al. 1976). If $GABA_A$ receptor antagonism and SK channel antagonism are the main contributors to the epileptogenic properties of BMI, supplying BMI to slices already perfused with PTX/apamin should result in little change to the oscillation. Instead, addition of BMI should generate a similar effect as adding slightly more apamin (because the concentration of apamin we used only partially blocked SK channels).

In the presence of 50 μM PTX and 1 nM apamin (a concentration that sufficiently replicated BMI), we applied 10 μM BMI (Fig. 5*A*; $n = 7$). As expected, BMI slightly but significantly prolonged the oscillation duration (5.6 ± 1.3 vs. 6.3 ± 1.2 s; paired *t*-test, $P < 0.05$) and increased the period (363 ± 7 vs. 391 ± 4 ms; paired *t*-test, $P < 0.001$) and number of spikes (1,323 ± 171 vs. 1,756 ± 156; paired *t*-test, $P < 0.001$). However, the OI was unchanged (0.87 ± 0.05 vs. 0.88 ± 0.06; paired *t*-test, $P > 0.05$). These results suggest

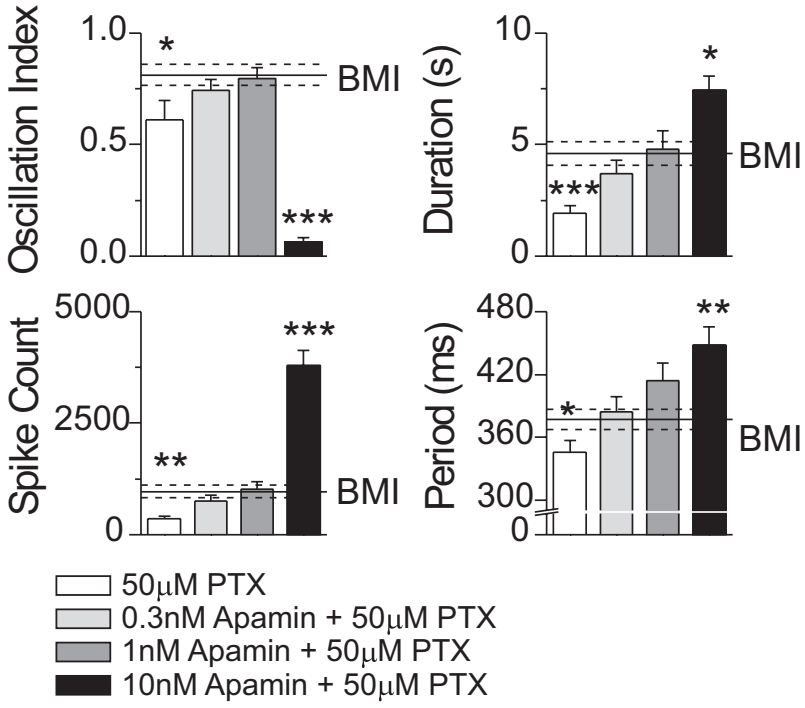

FIG. 4. $GABA_A$ receptor antagonism and partial SK channel blockade replicate robust BMI oscillations. *A*: quantification of evoked oscillations during PTX and apamin [0.3 ($n = 11$), 1 ($n = 11$), and 10 nM ($n = 4$)] coapplication. For reference, the horizontal lines show data for oscillations observed during BMI application (full line: mean; dotted lines: ±SE). Summary plots show the effect of 3 concentrations of apamin coapplied with PTX. Low concentrations of apamin (0.3 and 1 nM) did not produce significant differences compared with BMI for any of the 4 metrics, whereas a high concentration of apamin (10 nM) was significantly different on all 4 metrics (*t*-test: $*P < 0.05$; $**P < 0.01$; $***P < 0.001$).

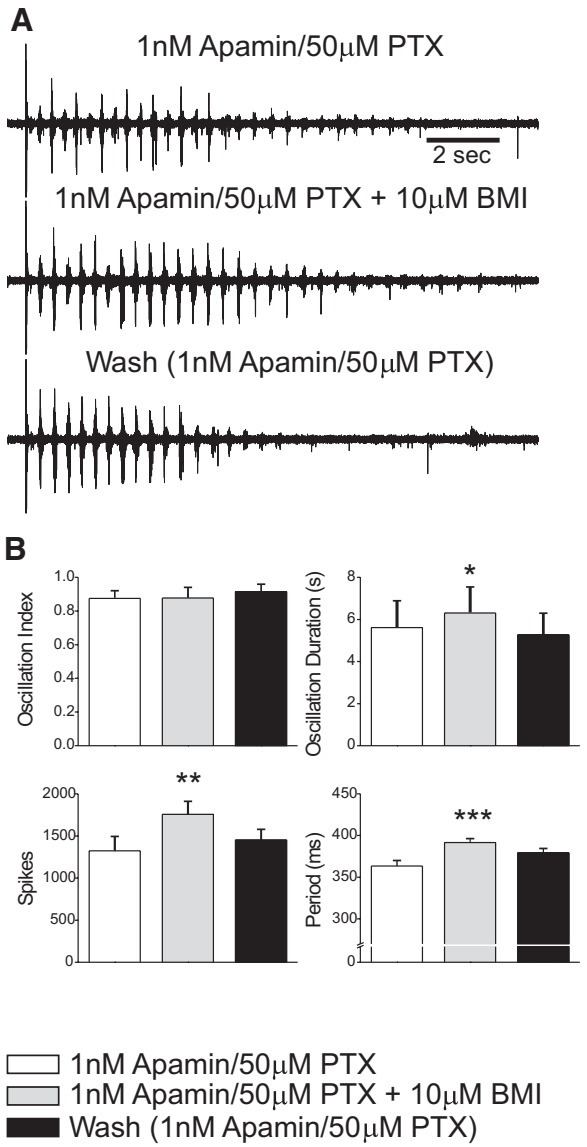

FIG. 5. Prior $GABA_A$ receptor and SK channel blockade largely occludes BMI-mediated transformation of thalamic oscillation. *A*: evoked oscillations during application of 50 μM PTX and 1 nM apamin (Control; top trace). BMI (10 μM) was added (BMI; middle trace) and washed out (Wash; bottom trace). All traces from the same slice. *B*: quantification of evoked oscillations in BMI, PTX, and apamin ($n = 7$) coapplication. Summary plots show the effect of BMI coapplied with PTX and apamin. Oscillations in BMI, PTX, and apamin were slightly but significantly longer, contained more spikes, and had a longer period than in PTX and apamin alone. However, BMI application did not result in changes to the oscillation index.

that, although BMI slightly enhances thalamic activity levels, the structure of the oscillation is not dramatically altered (i.e., no change in OI). Thus BMI does not seem to have significant pharmacological actions other than $GABA_A$ receptor and SK channel blockade.

Apamin enhances the intrinsic excitability of RT neurons but not relay neurons

Having shown that SK channels modulate both spike-wave and spindle-like oscillations, we probed the cellular mechanism of this change in both neuron subtypes involved in thalamic oscillations. Apamin might affect both a neuron's firing properties and its response to synaptic input. We focus on the former, which we refer to the neuron's intrinsic excitability. We recorded intracellularly from neurons in current-clamp mode. A family of short (400 ms) injections of hyperpolarizing and depolarizing current (−200 to 200 pA in 50-pA steps) were delivered to the relay neurons ($n = 6$; Fig. 6*A*). In general, a low threshold spike (LTS) crowned with action potentials followed hyperpolarizing current pulses greater than −100 pA (Fig. 6*A*), whereas depolarizing current pulses greater than +100 pA (Fig. 6*A, inset*) usually elicited an LTS followed by a train of regularly spaced action potentials (all action potentials were included in our analysis). Because postinhibitory rebound bursting in relay neurons is critical for generating thalamocortical oscillations (Huguenard and McCormick 2007), we were primarily interested in the spiking activity generated by hyperpolarizing pulses, which we report here. There was no change in the number of spikes or mean spike frequency of the rebound bursts in relay neurons. This result is consistent with both a low expression of SK2 channels in relay cells (Sailer et al. 2002, 2004) and a lack of T-type calcium channel and SK channel coupling (Kasten et al. 2007).

Because RT cells express a high density of SK channels (Sailer et al. 2004) and BMI is known to affect the intrinsic properties of these neurons (Debarbieux et al. 1998), we studied the effects of SK channel blockade on the intrinsic excitability of RT neurons. We recorded intracellularly from RT neurons in current-clamp mode in the presence of glutamate receptor antagonists to prevent network activity [DNQX (50 μM) and APV (100 μM)]. Short (400 ms) injections of hyperpolarizing and depolarizing current (−200 to 200 pA in 50-pA steps) were delivered to the RT neurons with the resting membrane potential held near −60 mV. Because RT cell firing is not affected by PTX (Debarbieux et al. 1998), we ran this protocol in both control conditions and during application of the three concentrations of apamin used for the oscillations (0.3, 1, and 10 nM). Because RT cells receive excitatory input during thalamocortical oscillations (Huguenard and McCormick 2007), we were particularly interested in the effect of apamin on bursts evoked by depolarizing current. Although we observed that apamin increased excitability at all levels of current injection, for simplicity we only report the effects at maximum current levels.

Similar to observations made while recording network oscillations, 0.3 ($n = 9$) and 1 nM ($n = 10$) apamin had relatively similar effects on the firing properties of RT cells, whereas 10 nM ($n = 6$) caused a much greater change in the evoked action potential activity. Partial blockade of SK channels by 0.3 or 1 nM apamin significantly enhanced the excitability of RT neurons (Fig. 7, *A* and *B*). Specifically, depolarizing current injections delivered during application of 0.3 or 1 nM apamin yielded more spikes (0.3 nM: 10 ± 1 vs. 14 ± 1, paired *t*-test, $P < 0.01$; 1 nM: 9 ± 1 vs. 17 ± 2, paired *t*-test, $P < 0.001$) and higher mean spike frequencies (0.3 nM: 27 ± 3 vs. 38 ± 3 Hz, paired *t*-test, $P < 0.01$; 1 nM: 27 ± 2 vs. 42 ± 7 Hz, paired *t*-test, $P < 0.01$) than in control conditions. Finally, 0.3 nM apamin and 1 nM apamin also increased the input resistance of RT neurons (0.3 nM: 132 ± 13 vs. 172 ± 11 MΩ, paired *t*-test, $P < 0.05$, 1 nM: 154 ± 10 vs. 184 ± 14 MΩ, paired *t*-test, $P < 0.05$). Apamin (10 nM) increased the number (control spikes: 9 ± 2, 10 nM: 27 ± 4; paired *t*-test, $P < 0.01$)

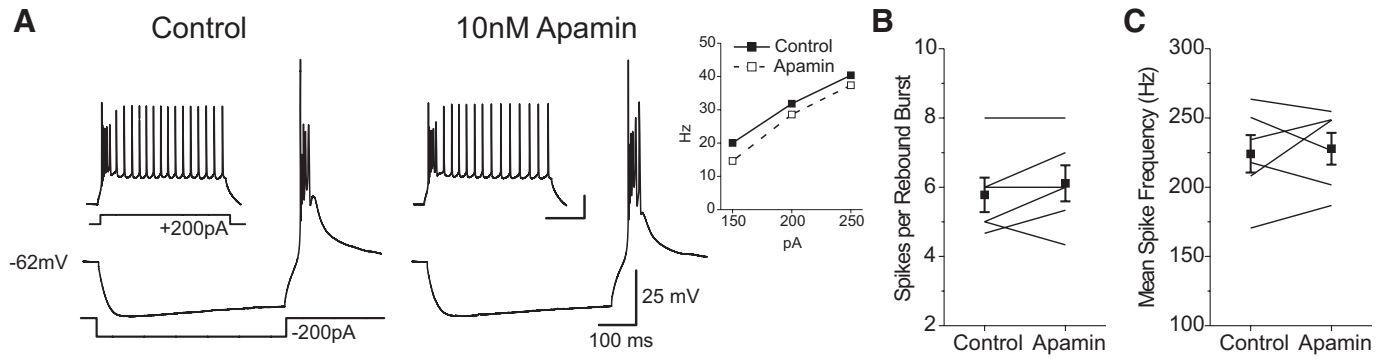

FIG. 6. Apamin has no effect on relay cell bursting. Hyperpolarizing and depolarizing current injection pulses (−200 to +200 pA in 50-pA steps) were delivered to relay neurons recorded in whole cell current-clamp configuration. *A*: an example whole cell current-clamp recording shows a rebound burst of action potentials following a hyperpolarizing current (−200 pA) in the same relay neuron. *Insets*: response to +200-pA current and a frequency current plot for the example neuron. Neither the number of spikes (*B*) nor the mean frequency (*C*) of a rebound burst following the termination of a maximally hyperpolarizing stimulus was changed in apamin. Each line represents a specific relay cell before and after application of apamin (filled symbol: mean ± SE; $n = 6$).

and mean frequency (control: 29 ± 5 Hz, 10 nM: 71 ± 10 Hz; paired *t*-test, $P < 0.01$) of action potentials elicited by 200pA of positive current (Fig. 7*C*). Additionally, 10 nM apamin significantly increased the input resistance of RT neurons (control: 135 ± 13 MΩ; 10 nM: 184 ± 14 MΩ; paired *t*-test, $P < 0.01$). Although it is likely that the observed increase in input resistance contributes to enhanced neuronal excitability, we did not directly test this possibility. Apamin (10 nM) also affected rebound bursts by prolonging the duration of the burst (control: 22.4 ± 4.9 ms, 10 nM: 81.5 ± 23.4 ms; paired *t*-test, $P < 0.05$), consistent with previous findings (Debarbieux et al. 1998). Apamin significantly increased the slope of a frequency-current plot (0.3 nM: 0.07 ± 0.03 vs. 0.20 ± 0.04, $P < 0.05$; 1 nM: 0.11 ± 0.01 vs. 0.21 ± 0.02, $P < 0.001$; 10 nM: 0.11 ± 0.03 vs. 0.51 ± 0.06, $P < 0.01$, paired *t*-test). Thus collectively, our data suggest that a selective enhancement of RT excitability likely mediates the effect of apamin on thalamic oscillations.

DISCUSSION

Main findings

To better understand the mechanisms underlying thalamocortical oscillations, we dissected the cause of hyperexcitability in the BMI model of absence epilepsy. In control conditions, the thalamic slice preparation generates sparse rhythmic activity reminiscent of spindle oscillations observed during non-REM sleep. We showed that both known actions of BMI, SK channel and $GABA_A$ receptor antagonism, transform these oscillations in vitro. Notably, SK channel antagonism slowed and prolonged oscillations generated both in control and PTX solutions, indicating the general importance of regulation of RT excitability in determining network function. The actions of BMI were replicated using a concentration of apamin (0.3–1 nM) that only partially blocks SK channels and a concentration of PTX (50 μM) that fully blocks $GABA_A$ receptors. Furthermore, BMI did not noticeably affect the oscillation through a non-SK channel/$GABA_A$ receptor mechanism. A higher concentration of apamin (10 nM) greatly prolonged the oscillation in both control and PTX. However, the oscillation became unsynchronized as some of the units fired continuously at this high concentration. Apamin had no effect on relay neurons but greatly enhanced the intrinsic excitability of RT neurons. This observation is consistent with previous localization data showing that SK channels are highly expressed in RT neurons (Debarbieux et al. 1998; Sailer et al. 2004) and that BMI affects RT cell burst firing (Debarbieux et al. 1998).

Synergy between enhanced intrinsic excitability and loss of inhibition in the RN

In vitro models of absence epilepsy suggest that multiple mechanisms in the thalamus limit the hyperexcitability of neurons in the reticular nucleus and prevent epileptiform network oscillations. BMI affects three distinct antioscillatory mechanisms in the thalamus (Fig. 8). *1*) $GABA_A$ receptor antagonism abolishes RT-RT neuron inhibition. Inhibition from neighboring RT cells can prevent neighboring cell bursting (Sohal and Huguenard 2003). Lifting this inhibition increases burst probability of individual RT neurons and, therefore enhances inhibition onto relay cells and promotes postinhibitory rebound bursting. Thus increasing feed-forward inhibition increases network excitability. Indeed, selective genetic knockout of inhibition between RT neurons seems to be sufficient for highly synchronized oscillations in mouse (Huntsman et al. 1999). *2*) BMI blocks short latency $GABA_A$ receptor–mediated inhibition onto relay neurons by blocking $GABA_A$ receptors. This action eliminates the heterogeneity associated with mixed $GABA_A$ and $GABA_B$ receptor–mediated inhibitory postsynaptic potentials (IPSPs; i.e., inhibition is only mediated by $GABA_B$ receptors). Because each relay cell normally receives a different balance of $GABA_A$ and $GABA_B$ receptor inhibition (Huguenard and Prince 1994), postinhibitory bursting times within the population of relay cells can vary substantially (Sohal et al. 2006; Ulrich and Huguenard 1996), thereby desynchronizing re-excitation of RT neurons and reducing the synchrony of the oscillation. Indeed, the inverse of this is also true in that blockade of $GABA_B$ receptors can enhance the synchrony of spindle oscillations (Jacobsen et al. 2001). *3*) BMI partially antagonizes SK channels in RT neurons, enhancing the intrinsic excitability of these neurons and likely causing greater GABA release from RT neuron terminals. At the RT-relay neuron synapse, greater concentrations of released GABA will activate a larger $GABA_B$ receptor–mediated component of the IPSP because of the peripheral localization of $GABA_B$ receptors on the synapse (Kulik et al. 2002). This action likely leads to less variable post inhibitory rebound

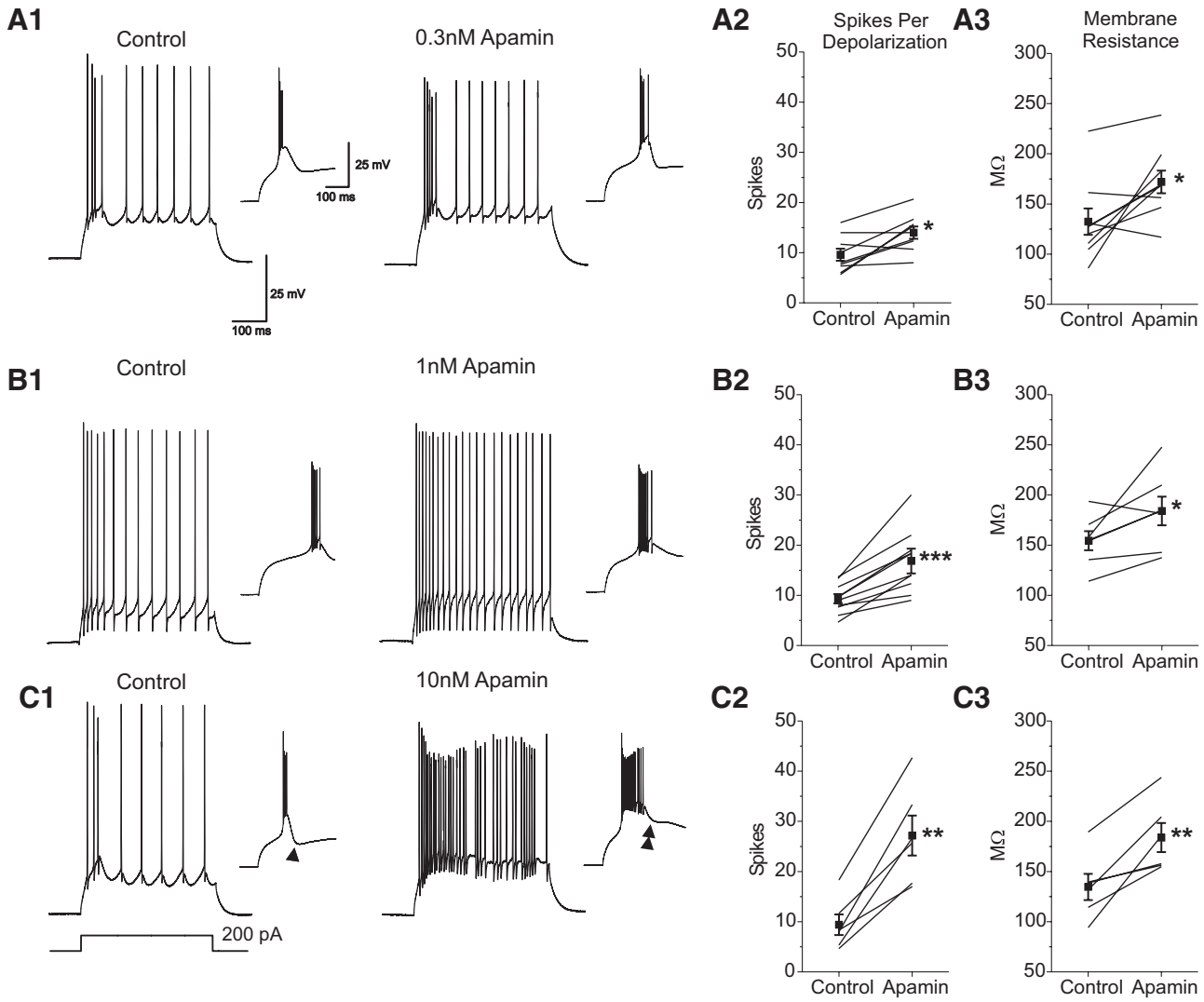

FIG. 7. Apamin enhances the intrinsic excitability of RT neurons. Four hundred-millisecond hyperpolarizing and depolarizing current injection pulses (−200 to +200 pA in 50-pA steps) were delivered to RT neurons recorded in the whole cell current-clamp configuration. The main panels in *A1–C1* show example responses to the maximum positive current injection (+200 pA) during 0.3 (*A*), 1 (*B*), and 10 nM (*C*) apamin application. Control and apamin recordings in each row are from the same neuron. *Insets*: rebound bursts of action potentials on termination of a −200-pA hyperpolarizing current. The number of spikes (*A2–C2*) elicited during the entire depolarizing current injection (both bursting and single spikes) and the membrane resistance (*A3–C3*) were compared between control and 0.3 (*A*; $n = 9$), 1 (*B*; $n = 10$), and 10 nM (*C*; $n = 6$) apamin application. Each line represents a different RT cell before and after application of apamin (filled symbol: mean ± SE). Arrowheads in *C1* indicate that afterhyperpolarization following burst in control conditions (single arrow) was reduced by apamin (double arrow). Scale bars in *A1* correspond to all intracellular recordings.

bursts (Fig. 8*B*) and thus enhanced synchrony (Debarbieux et al. 1998; Kim et al. 1997). Indeed enhanced simulated cortical feedback onto RT neurons during thalamic oscillations in vitro transforms the spindles into absence-like oscillations. This transformation is dependent on $GABA_B$ receptor activation. (Bal et al. 2000; Blumenfeld and McCormick 2000). Consistent with other studies (Avanzini et al. 1989; Cueni et al. 2008; Debarbieux et al. 1998), we show that RT neuron excitability is regulated by SK channels. Our findings show that this regulation likely modulates network oscillations.

Because apamin alone did not generate epileptiform oscillations characteristic of absence epilepsy, an enhancement of RT neuron excitability alone is not sufficient for highly synchronized oscillations. This finding suggests that when RT neuron excitability increases, inhibition between RT neurons also increases. Effectively, both feed-forward inhibition (pro-oscillatory) and intra-RT inhibition (antioscillatory) are scaled together, leading to increased activity that is none the less desynchronized.

The mechanism by which inhibition between RT cells desynchronizes thalamic oscillations is currently debated (Sanchez-Vives et al. 1997; Sohal and Huguenard 2003). Two hypotheses have been suggested: *1*) inhibition truncates bursts in RT cells or *2*) inhibition vetoes bursts in RT cells by making them less likely to fire a burst at all. Both of these mechanisms would reduce feedforward inhibition and thus lead to less robust oscillations. Our results support the burst veto hypothesis because application of apamin prolongs RT bursts (i.e., interferes with burst termination) but does not generate robust 3-Hz oscillations. It is important to note that blockade of $GABA_A$ receptors is unlikely to affect the intrinsic bursting properties of RT neurons be-

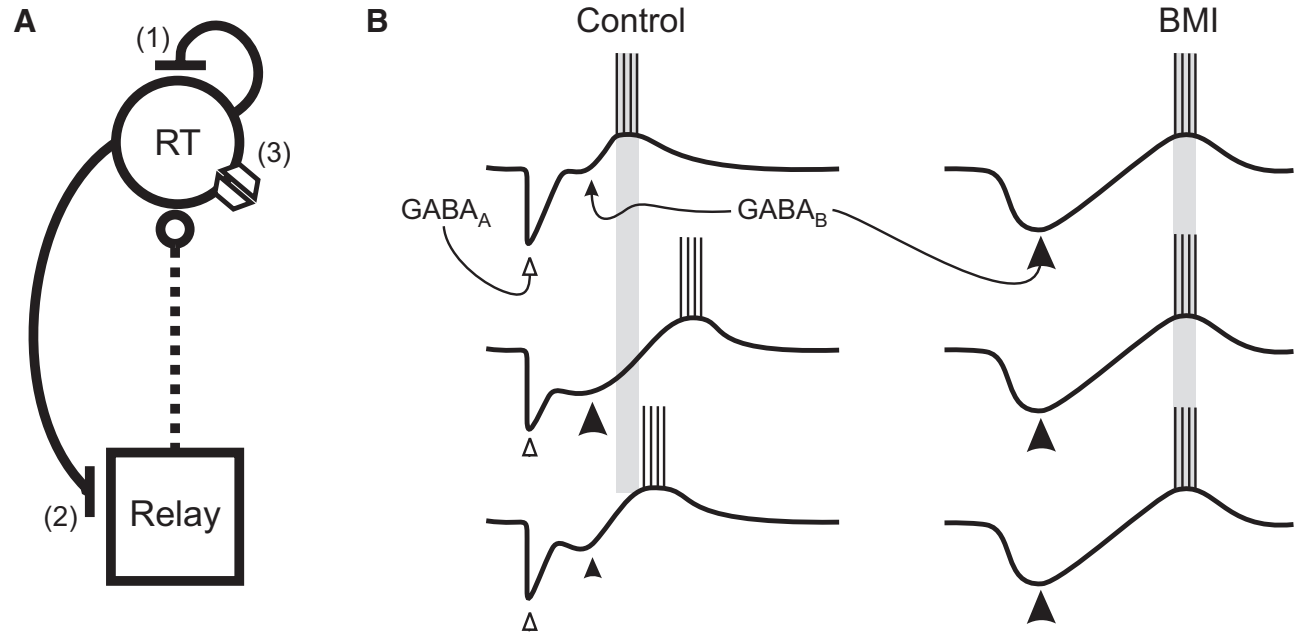

FIG. 8. Working model of BMI oscillations. Model proposing mechanisms underlying BMI-mediated transformation of thalamocortical oscillations. *A*: BMI generates a robust epileptiform oscillation through 3 mechanisms: *1*) blockade of inhibition between RT cells, *2*) homogenization of RT-relay inhibition through blockade of $GABA_A$ and enhanced activation of $GABA_B$ receptors, and *3*) partial blockade of SK channels. The schematic depicts a population of RT/relay neurons. *Mechanism 1* schematically represents RT inhibition of other RT neurons rather than true self-inhibition. *B*: the cartoon traces depict inhibitory postsynaptic potentials (IPSPs) mediated by different combinations of $GABA_A$ (open arrowheads)and $GABA_B$ (closed arrowheads) receptors in control conditions (*left*) and only $GABA_B$ receptors during BMI application (*right*). The size of the closed arrowhead corresponds to the magnitude of the $GABA_B$ IPSP. In control conditions, variable $GABA_A$ vs. $GABA_B$ IPSPs in individual cells promote heterogeneity in the timing of postinhibitory rebound bursts. Specifically, large $GABA_B$ IPSPs (e.g., middle control trace) result in long delays in postinhibitory rebound bursting relative to IPSPs with little/no $GABA_B$ component (e.g., top control trace). This heterogeneity is thought to be eliminated in the presence of BMI (Kim et al. 1997). The gray bars are aligned with the bursts of the top traces to show burst onset variability in control conditions and homogeneity of burst onset in BMI.

cause PTX does not affect RT cell bursting (Debarbieux et al. 1998). Thus in the BMI model, an enhancement in the intrinsic bursting properties of RT neurons is caused by partial SK channel blockade. However, although SK channel antagonism cannot generate epileptiform oscillations alone, it works synergistically in the presence of a $GABA_A$ receptor antagonist to create a robust oscillation.

Does some SK channel activity favor robust epileptiform oscillations?

The question remains as to what fraction of blocked SK channels maximally enhance oscillatory activity. We have shown that PTX generates relatively robust oscillations but not as robust as BMI. Low concentrations of apamin (0.3 or 1 nM) added to PTX generated more robust oscillations than PTX alone, an effect not observed when high concentrations of apamin (10 nM) were added to PTX. This suggests that partial blockade of SK channels is optimal for robust oscillations. However, the exact efficacy of apamin's blockade of SK channels in these neurons is unknown, complicating a tentative link between the extent of SK channel blockade and the OI. Moreover, because SK channel heteromer composition can determine apamin sensitivity (Benton et al. 2003) and all three SK genes are expressed in the RT (Sailer et al. 2004), quantitative calculation of the blockade is difficult. Heteromeric channels containing either SK1 or SK3 along with SK2 can result in decreased apamin sensitivity compared with SK2 alone. Further complicating this calculation is the observation that BMI blockade of SK channels is voltage dependent (Benton et al. 2003; Khawaled et al. 1999; Strobaek et al. 2000). Nonetheless, estimates of blockade efficacy can be made as follows. The SK channel-mediated current in RT neurons is not affected in SK1 knockout mice but is completely abolished in SK2 knockout mice (Cueni et al. 2008), suggesting that SK2-composed channels underlie our observed apamin effects. Based on the results from a heterologous expression system expressing only SK2 (Khawaled et al. 1999; Strobaek et al. 2000), we estimated the IC_{50} for apamin at 83 pM and the IC_{50} for BMI on SK channels at 1.7 μM at -60 mV. From these values, we estimate that 0.3, 1, and 10 nM apamin yield 78, 92, and 99% blockade, respectively. We further estimate that 10 μM BMI results in 86% SK channel blockade. The blockade efficacy of BMI falls between the putative efficacies for 0.3 and 1 nM apamin and is consistent with our results showing that the effects of BMI on oscillations could be replicated by 0.3 or 1 nM apamin combined with PTX. Thus partial blockade of SK channels leads to a maximally enhanced oscillation, whereas full blockade does not.

The hypothesis that partial SK channel blockade yields more robust oscillations than full blockade is supported by a recent analysis of a mouse lacking SK2 channels (Cueni et al. 2008), a condition analogous to complete pharmacological blockade of channel activity. Of particular relevance to our results, these knockout mice show a significant reduction in EEG spindle-related activity. These weaker oscillations are consistent with our observation that a theoretically complete block of SK channels resulted in a loss of oscillation synchrony. Three possible mechanisms might underlie this effect. *1*) RT neurons

can fire bursts lasting longer than the period of the oscillation (Debarbieux et al. 1998), which would prevent any recurrent excitation. *2*) Apamin-induced changes in RT neuron membrane resistance may reflect a significant depolarization of resting membrane potential and inactivation of the T-type calcium channels that mediate the RT burst firing required to sustain oscillatory activity (Huguenard and McCormick 2007). *3*) Increased spontaneous firing may enhance network refractoriness. Apamin (10 nM) resulted in high levels of background activity (tonic and burst firing) even in the absence of stimulation (personal observations). Future experiments will distinguish among these possibilities.

Implications for epilepsy

We showed here that limited SK channel antagonism generally promotes oscillatory thalamic network activity. This finding suggests the possibility that SK channel enhancement could have antioscillatory and potentially antiepileptic effects because SK channels limit RT neuronal excitability. Indeed, pharmacological SK channel openers such as 1-EBIO (which increases SK channel calcium sensitivity) can reduce the duration and intensity of seizures in certain animal seizure models (Anderson et al. 2006). It is interesting to speculate whether the anticonvulsant activity of SK channel activators would have a differential effect on various models of absence epilepsy. New advances in SK channel–positive modulators could also prove useful as antiepileptic agents (Hougaard et al. 2007). In the thalamus, these drugs may suppress epileptic (and other) oscillations by reducing the intrinsic excitability of RT neurons. Bidirectional regulation of SK channel calcium sensitivity by casein kinase 2 (CK2) and protein phosphatase 2A (PP2A) (Allen et al. 2007; Bildl et al. 2004) could also modulate thalamic oscillations in various physiological conditions.

Recent work has shown that surface expression and thus efficacy of SK channels can be dynamically regulated by protein kinase A (PKA) through NMDA receptor activation (Lin et al. 2008) or norepinephrine (Faber et al. 2008). Physiological activation of PKA in RT neurons may reduce SK channel expression, thus increasing intrinsic excitability of RT neurons and transforming the oscillatory network into a more excitable state. Furthermore, study of the developmental regulation of SK channels (Cingolani et al. 2002) may yield insights into the progression of childhood absence into adulthood. Future work on the modulation and function of SK channels in RT neurons may elucidate causative mechanisms as well as potential interventions for the childhood neurological disease absence epilepsy.

ACKNOWLEDGMENTS

We thank all the members of the Huguenard Laboratory for insightful discussion and technical guidance.

GRANTS

M. Kleiman-Weiner was funded by grants from the Irene and Eric Simon Brain Research Foundation and from Stanford Undergraduate Advising and Research. M. P. Beenhakker was funded through an Epilepsy Foundation Fellowship. This research was supported by National Institute of Neurological Disorders and Stroke Grant NS-034774.

REFERENCES

Allen D, Fakler B, Maylie J, Adelman JP. Organization and regulation of small conductance Ca^{2+}-activated K^+ channel multiprotein complexes. *J Neurosci* 27: 2369–2376, 2007.

Anderson NJ, Slough S, Watson WP. In vivo characterisation of the small-conductance KCa (SK) channel activator 1-ethyl-2-benzimidazolinone (1-EBIO) as a potential anticonvulsant. *Eur J Pharmacol* 546: 48–53, 2006.

Avanzini G, de Curtis M, Panzica F, Spreafico R. Intrinsic properties of nucleus reticularis thalami neurones of the rat studied in vitro. *J Physiol* 416: 111–122, 1989.

Bal T, Debay D, Destexhe A. Cortical feedback controls the frequency and synchrony of oscillations in the visual thalamus. *J Neurosci* 20: 7478–7488, 2000.

Benton DCH, Monaghan AS, Hosseini R, Bahia PK, Haylett DG, Moss GWJ. Small conductance Ca^{2+}-activated K^+ channels formed by the expression of rat SK1 and SK2 genes in HEK 293 cells. *J Physiol* 553: 13–19, 2003.

Bildl W, Strassmaier T, Thurm H, Andersen J, Eble S, Oliver D, Knipper M, Mann M, Schulte U, Adelman JP, Fakler B. Protein kinase CK2 is coassembled with small conductance Ca(2+)-activated K^+ channels and regulates channel gating. *Neuron* 43: 847–858, 2004.

Blumenfeld H, McCormick DA. Corticothalamic inputs control the pattern of activity generated in thalamocortical networks. *J Neurosci* 20: 5153–5162, 2000.

Castro-Alamancos MA. Neocortical synchronized oscillations induced by thalamic disinhibition in vivo. *J Neurosci* 19: RC27, 1999.

Cingolani LA, Gymnopoulos M, Boccaccio A, Stocker M, Pedarzani P. Developmental regulation of small-conductance ca^{2+}-activated k^+ channel expression and function in rat Purkinje neurons. *J Neurosci* 22: 4456–4467, 2002.

Cueni L, Canepari M, Lujan R, Emmenegger Y, Watanabe M, Bond CT, Franken P, Adelman JP, Luthi A. T-type Ca^{2+} channels, SK2 channels and SERCAs gate sleep-related oscillations in thalamic dendrites. *Nat Neurosci* 11: 683–692, 2008.

Debarbieux F, Brunton J, Charpak S. Effect of bicuculline on thalamic activity: a direct blockade of IAHP in reticularis neurons. *J Neurophysiol* 79: 2911–2918, 1998.

Faber ESL, Delaney AJ, Power JM, Sedlak PL, Crane JW, Sah P. Modulation of SK channel trafficking by beta adrenoceptors enhances excitatory synaptic transmission and plasticity in the amygdala. *J Neurosci* 28: 10803–10813, 2008.

Hougaard C, Eriksen BL, Jorgensen S, Johansen TH, Dyhring T, Madsen LS, Strobak D, Christophersen P. Selective positive modulation of the SK3 and SK2 subtypes of small conductance Ca^{2+}-activated K^+ channels. *Br J Pharmacol* 151: 655–665, 2007.

Huguenard JR, McCormick DA. Thalamic synchrony and dynamic regulation of global forebrain oscillations. *Trends Neurosci* 30: 350–356, 2007.

Huguenard JR, Prince DA. Intrathalamic rhythmicity studied in vitro: nominal T-current modulation causes robust antioscillatory effects. *J Neurosci* 14: 5485–5502, 1994.

Huntsman MM, Porcello DM, Homanics GE, DeLorey TM, Huguenard JR. Reciprocal inhibitory connections and network synchrony in the mammalian thalamus. *Science* 283: 541–543, 1999.

Jacobsen RB, Ulrich D, Huguenard JR. GABA(B) and NMDA receptors contribute to spindle-like oscillations in rat thalamus in vitro. *J Neurophysiol* 86: 1365–1375, 2001.

Kasten MR, Rudy B, Anderson MP. Differential regulation of action potential firing in adult murine thalamocortical neurons by Kv3.2, Kv1, and SK potassium and N-type calcium channels. *J Physiol* 584: 565–582, 2007.

Khawaled R, Bruening-Wright A, Adelman JP, Maylie J. Bicuculline block of small-conductance calcium-activated potassium channels. *Pfluegers Arch Eur J Physiol* 438: 314–321, 1999.

Kim U, Sanchez-Vives MV, McCormick DA. Functional dynamics of GABAergic inhibition in the thalamus. *Science* 278: 130–134, 1997.

Kulik A, Nakadate K, Nyiri G, Notomi T, Malitschek B, Bettler B, Shigemoto R. Distinct localization of GABA(B) receptors relative to synaptic sites in the rat cerebellum and ventrobasal thalamus. *Eur J Neurosci* 15: 291–307, 2002.

Lin MT, Lujan R, Watanabe M, Adelman JP, Maylie J. SK2 channel plasticity contributes to LTP at Schaffer collateral-CA1 synapses. *Nat Neurosci* 11: 170–177, 2008.

McCormick DA, Bal T. Sleep and arousal: thalamocortical mechanisms. *Annu Rev Neurosci* 20: 185–215, 1997.

McCormick DA, Contreras D. On the cellular and network bases of epileptic seizures. *Annu Rev Physiol* 63: 815–846, 2001.

Olsen RW, Ban M, Miller T. Studies on the neuropharmacological activity of bicuculline and related compounds. *Brain Res* 102: 283–299, 1976.

Pisani A, Bonsi P, Catania MV, Giuffrida R, Morari M, Marti M, Centonze D, Bernardi G, Kingston AE, Calabresi P. Metabotropic glutamate 2 receptors modulate synaptic inputs and calcium signals in striatal cholinergic interneurons. *J Neurosci* 22: 6176–6185, 2002.

Sailer CA, Hu H, Kaufmann WA, Trieb M, Schwarzer C, Storm JF, Knaus HG. Regional differences in distribution and functional expression of small-conductance Ca^{2+}-activated K^+ channels in rat brain. *J Neurosci* 22: 9698–9707, 2002.

Sailer CA, Kaufmann WA, Marksteiner J, Knaus HG. Comparative immunohistochemical distribution of three small-conductance Ca^{2+}-activated potassium channel subunits, SK1, SK2, and SK3 in mouse brain. *Mol Cell Neurosci* 26: 458–469, 2004.

Sanchez-Vives MV, Bal T, McCormick DA. Inhibitory interactions between perigeniculate GABAergic neurons. *J Neurosci* 17: 8894–8908, 1997.

Schumacher MA, Rivard AF, Bachinger HP, Adelman JP. Structure of the gating domain of a Ca^{2+}-activated K^+ channel complexed with Ca^{2+}/calmodulin. *Nature* 410: 1120–1124, 2001.

Sohal VS, Huguenard JR. Inhibitory interconnections control burst pattern and emergent network synchrony in reticular thalamus. *J Neurosci* 23: 8978–8988, 2003.

Sohal VS, Huntsman MM, Huguenard JR. Reciprocal inhibitory connections regulate the spatiotemporal properties of intrathalamic oscillations. *J Neurosci* 20: 1735–1745, 2000.

Sohal VS, Keist R, Rudolph U, Huguenard JR. Dynamic GABA(A) receptor subtype-specific modulation of the synchrony and duration of thalamic oscillations. *J Neurosci* 23: 3649–3657, 2003.

Sohal VS, Pangratz-Fuehrer S, Rudolph U, Huguenard JR. Intrinsic and synaptic dynamics interact to generate emergent patterns of rhythmic bursting in thalamocortical neurons. *J Neurosci* 26: 4247–4255, 2006.

Stocker M. Ca(2+)-activated K^+ channels: molecular determinants and function of the SK family. *Nat Rev Neurosci* 5: 758–770, 2004.

Strobaek D, Jorgensen TD, Christophersen P, Ahring PK, Olesen S-P. Pharmacological characterization of small-conductance Ca^{2+}-activated K^+ channels stably expressed in HEK 293 cells. *Br J Pharmacol* 129: 991–999, 2000.

Ulrich D, Huguenard JR. Gamma-aminobutyric acid type B receptor-dependent burst-firing in thalamic neurons: a dynamic clamp study. *Proc Natl Acad Sci USA* 93: 13245–13249, 1996.

von Krosigk M, Bal T, McCormick DA. Cellular mechanisms of a synchronized oscillation in the thalamus. *Science* 261: 361–364, 1993.